

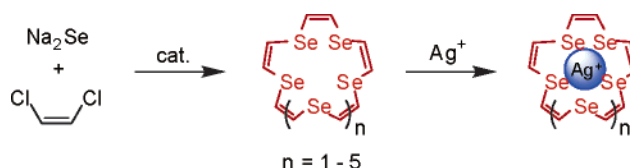
Unsaturated Selenacrown Ethers: Synthesis, Structure, and Formation of Silver Complexes

Toshio Shimizu, Mari Kawaguchi, Takahiro Tsuchiya, Kazunori Hirabayashi, and Nobumasa Kamigata*

Department of Chemistry, Graduate School of Science, Tokyo Metropolitan University, Minami-ohsawa, Hachioji, Tokyo 192-0397, Japan

kamigata-nobumasa@c.metro-u.ac.jp

Received February 11, 2005



The unsaturated selenacrown ethers, (*Z,Z,Z,Z,Z*)-1,4,7,10,13-pentaselecyclopentadeca-2,5,8,11,14-pentaene (15-US-5) (**2**), (*Z,Z,Z,Z,Z,Z*)-1,4,7,10,13,16-hexaselenacyclooctadeca-2,5,8,11,14,17-hexaene (18-US-6) (**3**), (*Z,Z,Z,Z,Z,Z,Z*)-1,4,7,10,13,16,19-heptaselecycloheneicosa-2,5,8,11,14,17,20-heptaene (21-US-7) (**4**), (*Z,Z,Z,Z,Z,Z,Z,Z*)-1,4,7,10,13,16,19,22-octaselecyclotetracos-2,5,8,11,14,17,20,23-octaene (24-US-8) (**5**), and (*Z,Z,Z,Z,Z,Z,Z,Z,Z*)-1,4,7,10,13,16,19,22,25-nonaselenacycloheptacos-2,5,8,11,14,17,20,23,26-nonaene (27-US-9) (**6**), were obtained together with 1,4-diselenin (**1**) by reacting sodium selenide with *cis*-dichloroethene in the presence of a phase-transfer catalyst. The crystal structures of **2–5** were determined by X-ray crystallographic analysis. The UV spectra of the selenacrown ethers showed absorption maximums in the range of 251–262 nm, which were assigned to $n \rightarrow \pi^*$ transitions. The cyclic voltammograms indicated that the large unsaturated selenacrown ethers were oxidized more easily than the small ones. The thermal reactions of the unsaturated selenacrown ethers afforded 1,4-diselenin (**1**) along with polymeric materials, whereas **1** was thermally stable even at 100 °C. The reactions of **1** or unsaturated selenacrown ethers **2–5** with silver ion yielded various novel silver complexes, $\text{Ag}(\text{C}_4\text{H}_4\text{Se}_2)(\text{CF}_3\text{COO})$ (**7**), $\text{Ag}(\text{C}_4\text{H}_4\text{Se}_2)_2(\text{CF}_3\text{COO})$ (**8**), $\text{Ag}(15\text{-US-5})(\text{CF}_3\text{COO})$ (**9**), $\text{Ag}_5(18\text{-US-6})_3(\text{CF}_3\text{COO})_5$ (**10**), $\text{Ag}_7(21\text{-US-7})(\text{CF}_3\text{COO})_5$ (**11**), $\text{Ag}(24\text{-US-8})_2(\text{CF}_3\text{COO})$ (**12**), $\text{Ag}_2(24\text{-US-8})(\text{CF}_3\text{COO})_2$ (**13**), $\text{Ag}_3(24\text{-US-8})_2(\text{CF}_3\text{COO})_3$ (**14**), $\text{Ag}(15\text{-US-5})\text{NO}_3$ (**15**), and $\text{Ag}(21\text{-US-7})\text{BF}_4$ (**16**). The stoichiometry for the complexation with silver trifluoroacetate in solution was examined by ^1H NMR measurement. The titration plots of **2** and **5** under the dilution conditions showed a distinct inflection point at the 1/1 metal/macrocyclic ratio, whereas the plots of **1** and **3** showed gradual change.

Introduction

Since the first report by Pedersen of the synthesis of crown ethers,¹ there has been tremendous development in the investigation of crown ethers, including thiocrown ethers.² Those studies have clarified that crown ethers have high affinity for alkali and alkaline earth metals,³ whereas thiocrown ethers are able to form stable com-

plexes with transition metals.⁴ Selenacrown ethers are also considered to be good ligands for transition metals.

(1) Pedersen, C. *J. Am. Chem. Soc.* **1967**, *89*, 7017.

(2) (a) *Crown Compounds: Toward Future Applications*; Cooper, R. S., Ed.; VCH Publishers: New York, 1992. (b) *Macrocyclic Synthesis: A Practical Approach*; Parker, D., Ed.; Oxford University Press: New York, 1996; Chapter 3. (c) Buter, J.; Kellogg, R. M. *Org. Synth.* **1987**, *65*, 150. (d) Wolf, R. E., Jr.; Hartman, J. R.; Ochrymowycz, L. A.; Cooper, S. R. *Inorg. Synth.* **1989**, *25*, 122. (e) Blower, P. J.; Cooper, S. R. *Inorg. Chem.* **1987**, *26*, 2009.

(3) (a) Izatt, R. M.; Bradshaw, J. S.; Nielsen, S. A.; Lamb, J. D.; Christensen, J. *J. Chem. Rev.* **1985**, *85*, 271. (b) Frensdorff, H. K. *J. Am. Chem. Soc.* **1971**, *93*, 600. (c) Gokel, G. W.; Goli, D. M.; Minganti, C.; Echegoyen, L. *J. Am. Chem. Soc.* **1983**, *105*, 6786. (d) Poonia, N. S. *J. Am. Chem. Soc.* **1974**, *96*, 1012.

(4) (a) Murray, S. G.; Hartley, F. R. *Chem. Rev.* **1981**, *81*, 365. (b) Blake, A. J.; Li, W.-S.; Lippolis, V.; Taylor, A.; Schröder, M. *J. Chem. Soc., Dalton Trans.* **1998**, 2931. (c) Blake, A. J.; Li, W.-S.; Lippolis, V.; Schröder, M. *J. Chem. Soc., Chem. Commun.* **1997**, 1943. (d) Blake, A. J.; Collison, D.; Gould, R. O.; Reid, G.; Schröder, M. *J. Chem. Soc., Dalton Trans.* **1993**, 521. (e) de Groot, B.; Loeb, S. *J. Inorg. Chem.* **1991**, *30*, 3103. (f) Blake, A. J.; Gould, R. O.; Holder, A. J.; Hyde, T. I.; Schröder, M. *Polyhedron* **1989**, *8*, 513. (g) Clarkson, J.; Yagbasan, R.; Blower, P. J.; Rawle, S. C.; Cooper, S. R. *J. Chem. Soc., Chem. Commun.* **1987**, 950. (h) Sekido, E.; Suzuki, K.; Hamada, K. *Anal. Sci.* **1987**, *3*, 505. (i) Pedersen, C. J. *J. Org. Chem.* **1971**, *36*, 254.

The synthesis of such selenacrown ethers⁵ as 16Se⁴⁶ has opened up the possibility of forming new complexes, and various metal complexes of selenacrown ethers have been reported.⁷ On the other hand, unsaturated crown ethers having cis carbon–carbon double bonds are considered to be more conformationally restricted than the corresponding saturated systems and are expected to display high selectivity for metals. The unsaturated crown ethers are classified into two categories: areno and nonareno. The areno crown ethers have been the subject of investigation since the beginning of crown ether chemistry. On the other hand, no nonareno crown ethers have been studied to date, except 1,4,7-trioxacyclononatriene⁸ and stilbenocrown ethers.⁹ Recently, we have synthesized simple unsaturated thiacycrown ethers with no carbon substituents and found that they have high selectivity for a number of ions and the kind of metals included in their cavities.^{10–12} From our studies of unsaturated thiacycrown ethers, we expect that unsaturated selenacrown ethers would exhibit different selectivities for the number and kind of metals due to differences in the electronegativities of the chalcogen atoms, the conformation, and the size of the cavities. However, no unsaturated selenacrown ethers possessing carbon–carbon double bonds have been synthesized so far. Herein, the syntheses and structures of unsaturated selenacrown ethers are reported together with the formation and inclusion behavior of the silver complexes.¹³

(5) (a) Hope, E. G.; Levason, W. *Coord. Chem. Rev.* **1993**, *122*, 109. (b) Levason, W.; Orchard, S. D.; Reid, G. *Coord. Chem. Rev.* **2002**, *225*, 159.

(6) Batchelor, R. J.; Einstein, F. W. B.; Gay, I. D.; Gu, J.-H.; Johnston, B. D.; Pinto, B. M. *J. Am. Chem. Soc.* **1989**, *111*, 6582.

(7) (a) Kumagai, T.; Akabori, S. *Chem. Lett.* **1989**, 1667. (b) Li, W.-P.; Liu, X.-F.; Xu, H.-S. *Acta Chim. Sin.* **1994**, *52*, 1082. Levason, W.; Reid, G.; Smith, S. M. *Polyhedron* **1997**, *16*, 4253. (c) Levason, W.; Quirk, J. J.; Reid, G.; Smith, S. M. *J. Chem. Soc., Dalton Trans.* **1997**, 3719. (d) Levason, W.; Quirk, J. J.; Reid, G. *J. Chem. Soc., Dalton Trans.* **1996**, 3713. (e) Kelly, P. F.; Levason, W.; Reid, G.; Williams, D. J. *J. Chem. Soc., Chem. Commun.* **1993**, 1716. (f) Davies, M. K.; Levason, W.; Reid, G. *J. Chem. Soc., Dalton Trans.* **1998**, 2185. (g) Batchelor, R. J.; Einstein, F. W. B.; Gay, I. D.; Gu, J.-H.; Pinto, B. M.; Zhou, X.-M. *Inorg. Chem.* **1996**, *35*, 3667. (h) Levason, W.; Quirk, J. J.; Reid, G. *Inorg. Chem.* **1994**, *33*, 6120. (i) Champness, N. R.; Kelly, P. F.; Levason, W.; Reid, G.; Slawin, A. M. Z.; Williams, D. J. *Inorg. Chem.* **1995**, *34*, 651. (j) Batchelor, R. J.; Einstein, F. W. B.; Gay, I. D.; Gu, J.-H.; Pinto, B. M. *J. Organomet. Chem.* **1991**, *411*, 147. (k) Batchelor, R. J.; Einstein, F. W. B.; Gay, I. D.; Gu, J.-H.; Pinto, B. M.; Zhou, X.-M. *J. Am. Chem. Soc.* **1990**, *112*, 3706. (l) Batchelor, R. J.; Einstein, F. W. B.; Gay, I. D.; Gu, J.-H.; Pinto, B. M.; Zhou, X.-M. *Can. J. Chem.* **2000**, *78*, 598. (m) Booth, D. G.; Levason, W.; Quirk, J. J.; Reid, G.; Smith, S. M. *J. Chem. Soc., Dalton Trans.* **1997**, 3493. (n) Hill, N. J.; Levason, W.; Reid, G. *Inorg. Chem.* **2002**, *41*, 2070. (o) Barton, A. J.; Hill, N. J.; Levason, W.; Reid, G. *J. Am. Chem. Soc.* **2001**, *123*, 11801. (p) Barton, A. J.; Hill, N. J.; Levason, W.; Reid, G. *J. Chem. Soc., Dalton Trans.* **2001**, 1621. (q) Barton, A. J.; Hill, N. J.; Levason, W.; Patel, B.; Reid, G. *J. Chem. Soc., Chem. Commun.* **2001**, 95. (r) Barton, A. J.; Genge, A. R. J.; Levason, W.; Reid, G. *J. Chem. Soc., Dalton Trans.* **2000**, 2163.

(8) Schwesinger, R.; Fritz, H.; Prinzbach, H. *Chem. Ber.* **1979**, *112*, 3318.

(9) (a) Merz, A. *Angew. Chem., Int. Ed. Engl.* **1977**, *16*, 467. (b) Inoue, Y.; Harino, H.; Nakazato, T.; Hakushi, T. *J. Org. Chem.* **1985**, *50*, 5151.

(10) Tsuchiya, T.; Shimizu, T.; Kamigata, N. *J. Am. Chem. Soc.* **2001**, *123*, 11534.

(11) Tsuchiya, T.; Shimizu, T.; Hirabayashi, K.; Kamigata, N. *J. Org. Chem.* **2002**, *67*, 6632.

(12) Tsuchiya, T.; Shimizu, T.; Hirabayashi, K.; Kamigata, N. *J. Org. Chem.* **2003**, *68*, 3480.

(13) Preliminary communication: Shimizu, T.; Kawaguchi, M.; Tsuchiya, T.; Hirabayashi, K.; Kamigata, N. *Org. Lett.* **2003**, *5*, 1443.

Results and Discussion

Synthesis of Unsaturated Selenacrown Ethers.

Treatment of *cis*-dichloroethene with sodium selenide, prepared from selenium, sodium hydroxide, and Rongalit,¹⁴ in acetonitrile in the presence of 0.1 equiv of 15-crown-5 yielded 1,4-diselenin (**1**) and 15-, 18-, 21-, 24-, and 27-membered unsaturated selenacrown ethers (15-US-5, 18-US-6, 21-US-7, 24-US-8, and 27-US-9, respectively)¹⁵ **2–6** in 29% total yield with a 24/6/22/20/16/12 product ratio of **1–6** (Scheme 1). Compounds **1–6** were isolated by silica gel column chromatography (hexane/acetone = 2/1) and gel permeation chromatography (chloroform). The use of 0.05 equiv of 15-crown-5 as the phase-transfer catalyst brought upon a decline of the yield, and no improvement was observed when 0.3 equiv of 15-crown-5 was added, as shown in Table 1.

No 9- and 12-membered unsaturated selenacrown ethers were obtained in the above reactions. This may be due to the unfavorable configuration during the ring closure reaction. The relative energies of the 9- and 12-membered unsaturated selenacrown ethers were compared to those of **1–6** using ab initio molecular orbital calculations, as the configuration during the ring closure reaction is considered to be strongly influenced by the conformation and strain of the products. Geometries were optimized using the Hartree–Fock (HF) method with the LANL2DZ basis set. X-ray structures of **2–5**, as described later, were used as the initial guesses, and those of 9-, 12-, and 27-membered cyclic compounds were calculated from some possible geometries. The final energies were calculated using the second-order Møller–Plesset perturbation (MP2) method for the HF geometries. The relative energy of one C₂H₂Se unit in these molecules,

SCHEME 1. Synthesis of Unsaturated Selenacrown Ethers

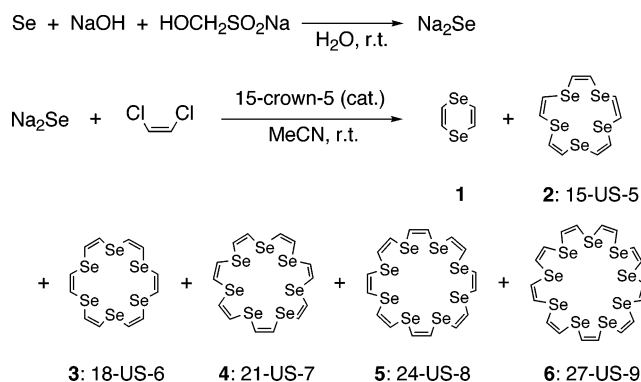


TABLE 1. Synthesis of Unsaturated Selenacrown Ethers^a

run	15-crown-5 (equiv)	total (%)	yield ^b						
			1	2	3	4	5	6	
1		0.012	/	/	39	/	61	/	/
2	0.05	16	7	/	12	/	27	/	22
3	0.1	29	24	/	6	/	22	/	20
4	0.3	23	19	/	3	/	20	/	22

^a Reactions were carried out in acetonitrile at room temperature.

^b Yields and ratios were determined by ¹H NMR measurement after removal of polymeric products.

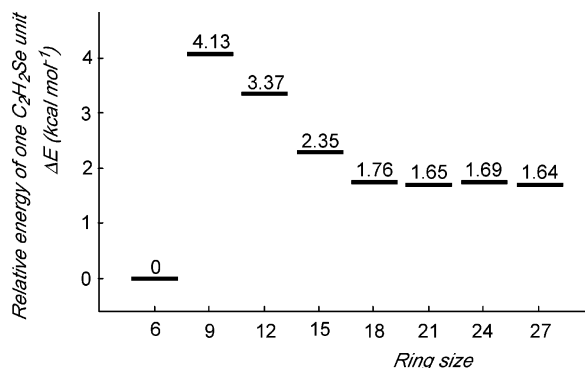


FIGURE 1. Calculated relative energies (kcal mol⁻¹) of one C₂H₂Se unit of 9-US-3, 12-US-4, and 1–6.

as shown in Figure 1, may reflect the strain energy of one C₂H₂Se unit, as all of these molecules have similar bonding characteristics. From these calculations, it was found that the relative energies of the 9- and 12-membered compounds were higher than those of the other selenacrown ethers. This unfavorable energy situation of the C₂H₂Se unit is likely to be the cause of the lack of formation of the 9- and 12-membered cyclic compounds in the reaction.

Crystal Structures of Unsaturated Selenacrown Ethers. The crystal structures of unsaturated selenacrown ethers **2**,¹³ **3**,¹³ **4**, and **5** were determined by X-ray crystallographic analysis, as shown in Figure 2. The bond lengths and angles are almost normal for all of the compounds. The crystal structures of **2–5** indicate that all of the olefin moieties have cis geometry and all of the selenium atoms lie almost on their respective planes. The most interesting point in the structures of **2–5** is the shape and size of the cavity. The cavities of large unsaturated selenacrown ethers are elliptically slender, whereas the structures of the corresponding unsaturated thiacycrown ethers become rounder with increasing ring size.¹⁰ The longest widths of the cavities surrounded by selenium atoms of **3–5** are 3.41, 5.98, and 8.36 Å, respectively, whereas the shorter ones are 1.16, 1.05, and 1.40 Å.

NMR Spectra of Unsaturated Selenacrown Ethers. Each of the ¹H and ¹³C NMR spectra of 1–6 showed a singlet, indicating that 1–6 exhibit flexibility to some extent in solution. The ¹H and ¹³C NMR signals were shifted upfield with increasing ring size for 2–6 in CDCl₃ {¹H NMR (ppm): **2**, 7.16; **3**, 7.12; **4**, 7.09; **5**, 7.08; **6**, 7.06. ¹³C NMR (ppm): **2**, 127.0; **3**, 125.7; **4**, 124.8; **5**, 124.3; **6**, 123.8}. On the other hand, the ⁷⁷Se NMR signals were shifted downfield with increasing ring size {⁷⁷Se NMR (ppm): **2**, 336.5; **3**, 350.1; **4**, 353.7; **5**, 354.9; **6**, 357.7}. These results suggest that the electron density of the olefin moieties is increased and that of selenium is decreased with increasing ring size of the unsaturated selenacrown ethers. The chemical shifts of 1–6 on the ¹H NMR spectra were also found at lower fields than those of the corresponding sulfur analogues, whereas those on the ¹³C NMR spectra were almost the same as those of the sulfur analogues.¹⁰

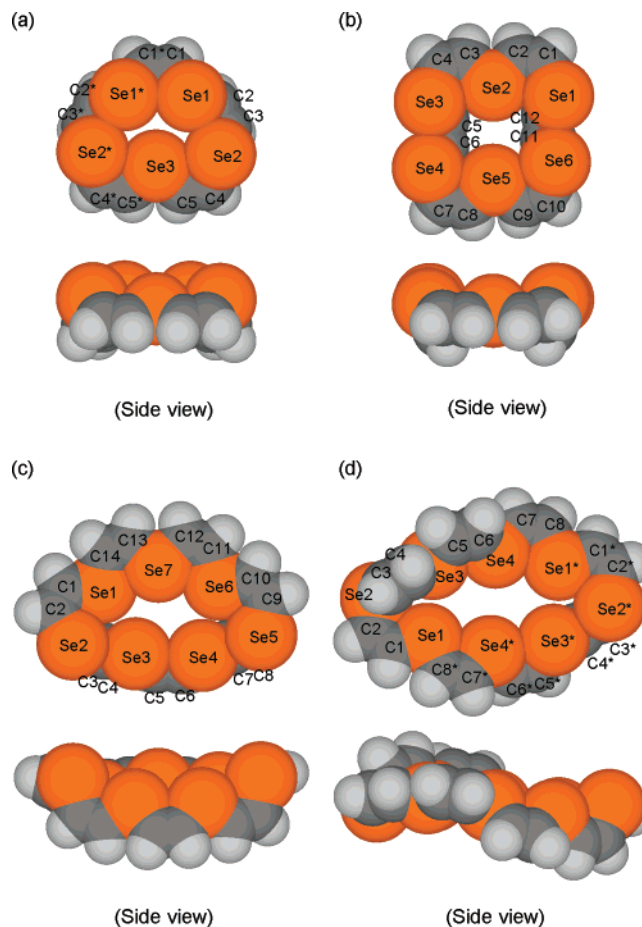


FIGURE 2. Crystal structures of (a) 15-US-5 (**2**), (b) 18-US-6 (**3**), (c) 21-US-7 (**4**), and (d) 24-US-8 (**5**) showing van der Waals radii.

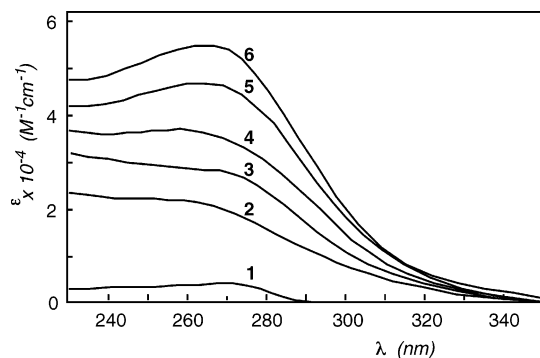


FIGURE 3. UV spectra of 1,4-diselenin (**1**), 15-US-5 (**2**), 18-US-6 (**3**), 21-US-7 (**4**), 24-US-8 (**5**), and 27-US-9 (**6**) in dichloromethane.

UV Spectra of Unsaturated Selenacrown Ethers. The UV spectrum of **2** showed an absorption maximum at 260 nm in dichloromethane (Figure 3). Compounds **3–6** also showed absorption maxima in the similar region. The extinction coefficients were increased with increasing ring size. The absorption maxima of 1–6 were also found to shift to longer wavelengths with decreasing solvent polarity, as shown in Table 2, indicating that the absorptions are assigned to n→π* transitions.

(14) Bird, M. L.; Challenger, F. J. *Chem. Soc.* **1942**, 570.

(15) In this paper, unsaturated selenacrown ethers are abbreviated as *x*-US-*y* (US, unsaturated selenacrown ether; *x*, *x*-membered ring; *y*, number of selenium atoms).

TABLE 2. UV Spectral Data of 1–6 in Various Solvents

compd	λ_{\max}/nm ($\epsilon \times 10^{-4}/\text{M}^{-1} \text{cm}^{-1}$)			
	MeCN	EtOH	CH ₂ Cl ₂	C ₆ H ₁₂
1	269 (0.5)	271 (0.5)	274 (0.4)	272 (0.5)
2	252 (2.0)	259 (1.5)	260 (2.2)	261 (2.2)
3	262 (2.7)	266 (1.9)	269 (2.8)	271 (–) ^a
4	251 (3.8)	253 (3.1)	256 (3.7)	266 (–) ^a
5	254 (5.0)	261 (3.9)	262 (4.7)	269 (–) ^a
6	256 (5.8)	262 (4.6)	264 (5.5)	271 (–) ^a

^a Molar absorption coefficient was not determined due to insolubility, and the spectra were measured in saturated solutions.

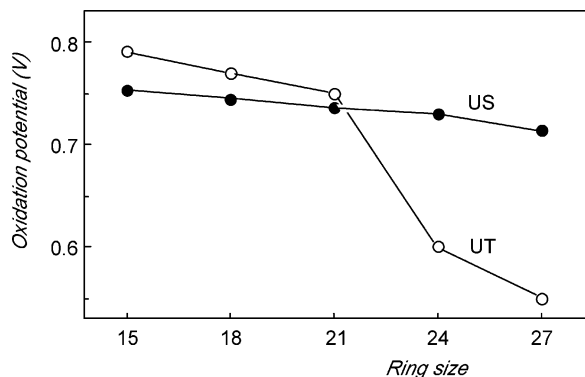


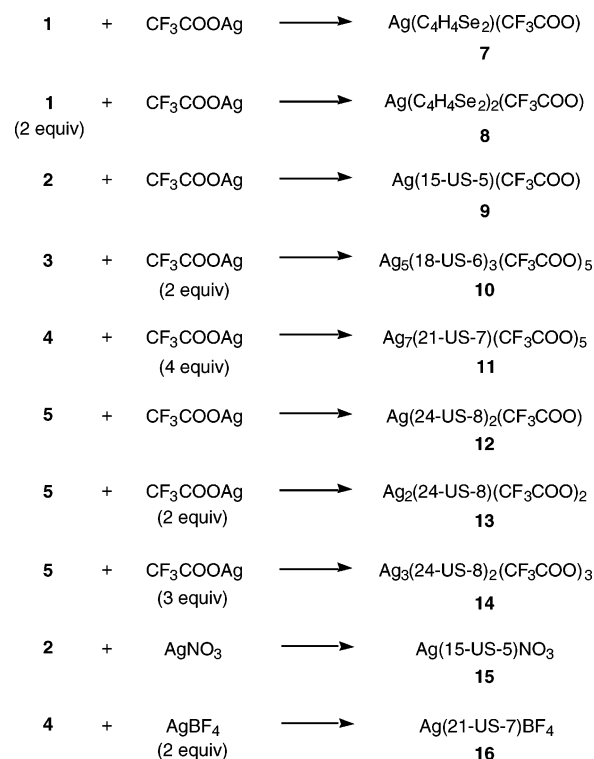
FIGURE 4. Oxidation potential of unsaturated selenacrown (US) and thiacrown (UT) ethers.

Electrochemistry of Unsaturated Selenacrown Ethers. Unsaturated selenacrown ethers 2–6 showed irreversible cyclic voltammograms. The potential was scanned at 100 mV/s versus Fc/Fc⁺ toward the cathodic direction and back again. Single oxidation peaks were observed at +0.752 (2), +0.743 (3), +0.736 (4), +0.729 (5), and +0.714 V (6), indicating that the large unsaturated selenacrown ethers are more easily oxidized than the small ones perhaps due to the delocalization effect of the resulting cation. The cyclic voltammogram of 1 showed pseudo reversible redox potential at $E_{1/2} = +0.436$ V ($\Delta E = 0.100$ V) and a second oxidation peak at +1.042 V vs Fc/Fc⁺, indicating stabilization by the 6 π electron system in the resulting dication.

The oxidation potential of the unsaturated selenacrown (US) ethers was almost constant, whereas that of the unsaturated thiacrown (UT) ethers was markedly changed among the 21- and 24-membered cyclic systems (Figure 4).¹⁰ This may be due to structural differences between the unsaturated selenacrown ethers and the thiacrown ethers; 2–5 exhibited stable elliptically slender conformations, whereas the unsaturated thiacrown ethers became rounder with increasing ring size,¹⁰ and the resulting cations of the unsaturated thiacrown ethers with large ring size may be well stabilized by the resonance between sulfurs and olefin moieties.

Thermal Stability of Unsaturated Selenacrown Ethers. The thermal stability of 2–5 was examined at 100 °C in CDCl₃. Selenacrown ethers 2–5 showed percentage decomposition of 75%, 77%, 93%, and 60%, respectively, after 8 d, to give 30%, 47%, 39%, and 21% conversion yields of 1,4-diselenin (1). Similarly, in DMSO-d₆ at 100 °C, 2–5 showed percentage decomposition of 92%, 100%, 87%, and 86%, respectively, after 8 d, yielding

SCHEME 2. Formation of Silver Complexes of Unsaturated Selenacrown Ethers



28%, 25%, 26%, and 29% of 1. 1,4-Diselenin 1 was stable under these conditions. To compare the stability of the unsaturated selenacrown ethers with that of the unsaturated thiacrown ethers, the thermal reaction of 15- and 18-membered unsaturated thiacrown ethers (15-UT-5 and 18-UT-6) was examined. Unsaturated thiacrown ethers 15-UT-5 and 18-UT-6 did not decompose at 100 °C in these solvents, whereas they decomposed to yield 1,4-dithiin and polymeric materials at 140 °C. Thus, the unsaturated selenacrown ethers were found to be thermally less stable than their corresponding sulfur analogues, probably because of their weak carbon–selenium bonds as compared to the carbon–sulfur bonds.

Complexation of Unsaturated Selenacrown Ethers with Silver Ion. The reactions of 1 and 2 equiv of 1 with silver trifluoroacetate in acetone at room temperature yielded Ag(C₄H₄Se₂)(CF₃COO) (7) and Ag(C₄H₄Se₂)₂(CF₃COO) (8), respectively (Scheme 2). The reaction of 2 with 1 equiv of silver trifluoroacetate afforded Ag(15-US-5)(CF₃COO) (9) as a colorless solid. Similarly, the reaction of 3 with 2 equiv of silver trifluoroacetate yielded Ag₅(18-US-6)₃(CF₃COO)₅ (10) as a yellow solid, whereas the reaction of 3 with 1 equiv of silver trifluoroacetate did not afford a stable complex. Ag₇(21-US-7)(CF₃COO)₅ (11) was obtained by adding 4 equiv of silver trifluoroacetate to an acetone solution of 4. Yellow prisms of 11 were precipitated from the hexane–acetone solution. The complexation reactions of 5 with 1, 2, and 3 equiv of silver trifluoroacetate afforded Ag(24-US-8)₂(CF₃COO) (12), Ag₂(24-US-8)(CF₃COO)₂ (13), and Ag₃(24-US-8)₂(CF₃COO)₃ (14), respectively, as colorless solids. The complex of 2 with silver nitrate, Ag(15-US-5)NO₃ (15), and that of 4 with silver tetrafluoroborate, Ag(21-US-7)BF₄ (16), were also obtained by respective reactions.

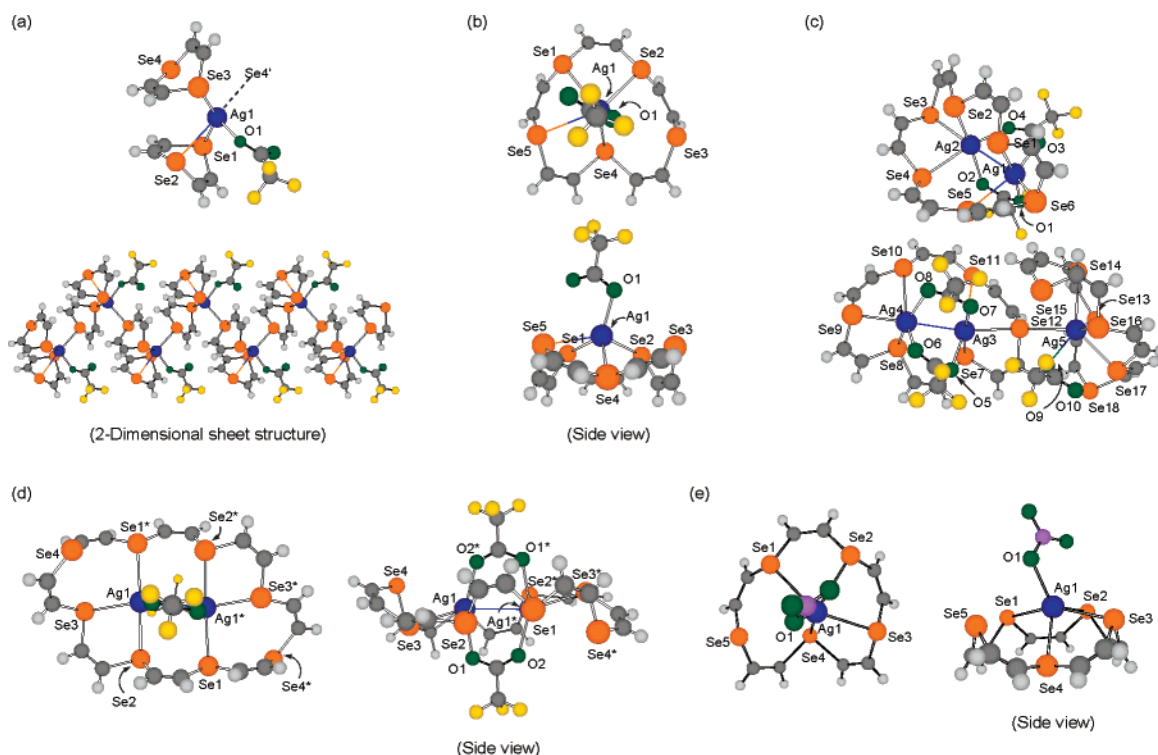


FIGURE 5. Crystal structures of (a) $\text{Ag}(\text{C}_4\text{H}_4\text{Se}_2)_2(\text{CF}_3\text{COO})$ (**8**), (b) $\text{Ag}(15\text{-US-5})(\text{CF}_3\text{COO})$ (**9**), (c) $\text{Ag}_5(18\text{-US-6})_3(\text{CF}_3\text{COO})_5$ (**10**), (d) $\text{Ag}_2(24\text{-US-8})(\text{CF}_3\text{COO})_2$ (**13**), and (e) $\text{Ag}(15\text{-US-5})\text{NO}_3$ (**15**).

Crystal Structures of Silver Complexes with Unsaturated Selenacrown Ethers. The crystal structures of silver complexes **8**, **9**, **10**,¹³ **13**, and **15** were determined by X-ray crystallographic analysis, as shown in Figure 5.

The crystal structure of **8** showed three or four selenium atoms coordinating to a silver atom. It was also found that the crystal formed a two-dimensional sheet structure through the coordination of Ag1 with Se4' of a neighboring lattice.

The ORTEP drawing of **9** revealed that one silver atom is present in the macrocycle cavity, and three selenium atoms {Se1, Se2, and Se4} coordinate to the silver atom {Ag1–Se1 2.81, Ag1–Se2 2.82, Ag1–Se4 2.73 Å}. Moreover, Se5 is located close to Ag1 with a distance of 3.08 Å. The angles Se1–Ag1–Se2, Se2–Ag1–Se4, Se4–Ag1...Se5, and Se5...Ag1–Se1 measured 78.6°, 98.5°, 73.7°, and 70.7°, respectively, and the angles O1–Ag1–Se1, O1–Ag1–Se2, O1–Ag1–Se4, and O1–Ag1...Se5 measured 126.4°, 107.5°, 122.8°, and 107.3°, respectively. Thus, the geometry around the silver atom has a distorted five-coordinate square pyramidal arrangement. The crystal structure of **15** is similar to that of **9**.

The crystal structure of **10**, which is composed of three crown subunits, revealed that one 18-US-6 unit coordinates to one silver atom and the other two units coordinate to two silver atoms. In the case of the corresponding unsaturated thiocrown ether (18-UT-6), a 1/1 complex was obtained as stable crystals.¹¹ These results indicate that the cavity size of **3** is larger than that of 18-UT-6, and **3** can coordinate to the two silver atoms in the cavity. The ¹H NMR spectrum of complex **10** in solution showed only one singlet, indicating that there is facile intercon-

version between $\text{Ag}(18\text{-US-6})(\text{CF}_3\text{COO})$ and $\text{Ag}_2(18\text{-US-6})(\text{CF}_3\text{COO})_2$ in solution.

The crystal structure of **13** showed that two silver atoms are present in the cavity of one 24-US-8 unit. The two trifluoroacetate groups are located at the opposite sides of the ring plane, and two oxygen atoms of each trifluoroacetate group coordinate to different silver atoms. Se1*, Se2, and Se3 coordinate to Ag1, and Se1, Se2*, and Se3* coordinate to Ag1*. The distance between Ag1 and Ag1* is 3.13 Å, which is smaller than twice the van der Waals radius for silver (3.96 Å) and nearly twice the covalent radius (2.88 Å).

Silver Ion Inclusion Behavior of Unsaturated Selenacrown Ethers in Solution. The inclusion behavior of unsaturated selenacrown ethers in solution was examined to confirm whether the silver complexes obtained as crystals were the only structures in solution or they could be isolated because of good crystallinity. The ¹H NMR spectra of complexes **7–16** measured in acetone-*d*₆ showed only one singlet each, although specific selenium atoms coordinate to the silver atom in the crystalline states of **8–10**, **13**, and **15**. These results indicate that there is facile interconversion between the complexing and noncomplexing macrocycles in solution. The inclusion behavior in solution was examined as follows: ¹H NMR spectra of the unsaturated selenacrown ethers were measured in acetone-*d*₆ at the concentration of 2.0 mM in the presence of 0–7 molar equiv of silver trifluoroacetate, and the difference between the observed chemical shift and that of the host molecule was plotted versus the relative concentration of the silver ion. The signal in the ¹H NMR spectra of **1–5** was shifted downfield with increasing molar equiv of silver tri-

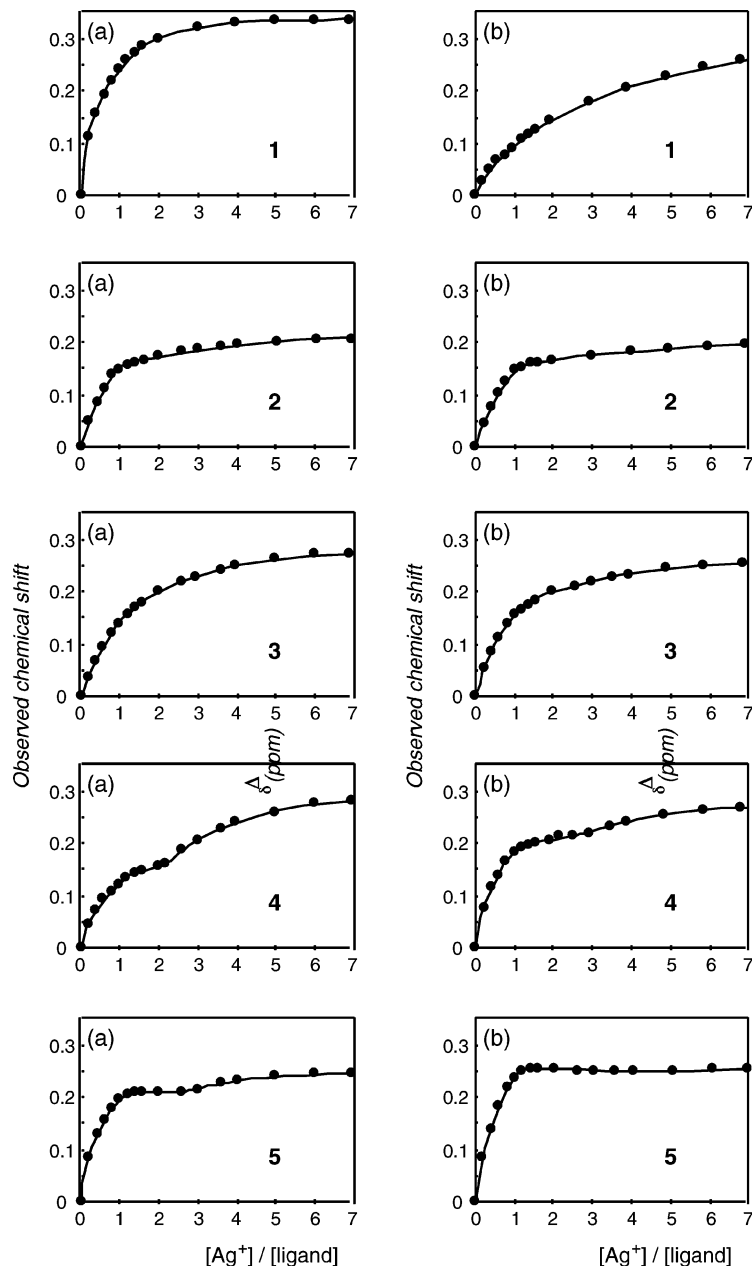


FIGURE 6. ^1H NMR titration plots of **1–5** with silver trifluoroacetate in acetone- d_6 . Concentrations of the ligands are (a) 2.0 mM and (b) 0.2 mM.

fluoroacetate {Figure 6a}. Although the titration plot of **1** did not show any remarkable behavior, that of **2** showed a linear change up to 1 equiv of silver ion, followed by a near-plateau at $[\text{Ag}^+]/[\mathbf{2}] = 1/1$. In the case of **3**, there was no remarkable change in the slope. In the case of **4**, the slope had an inflection point at $[\text{Ag}^+]/[\mathbf{4}] = 2/1$, indicating that there are more than two kinds of silver complexes in solution even though only 7/1 ($\text{Ag}^+/\mathbf{21}$ -US-7) complex **11** was obtained as a solid. Similarly, in the case of **5**, the titration curve showed some inflection points, indicating the presence of several kinds of complexes in solution. This result may correspond to the three kinds of Ag complexes of **5** obtained as crystals, and these behaviors may be attributed to the flexible conformation of large macrocycles.

To obtain the binding constants of **1–5**, the same experiment was performed under dilution conditions (0.2

mM) {Figure 6b}. The binding constants of **1–5** with silver trifluoroacetate were determined by a nonlinear least-squares fit of the second-order equilibrium equation to the titration plots of **1–5**. The K_1 and K_2 values of **1** and **5** were calculated from equations $\text{L} + \text{M} \rightarrow \text{LM}$ and $\text{LM} + \text{L} \rightarrow \text{L}_2\text{M}$, and those of **2–4** were calculated from $\text{L} + \text{M} \rightarrow \text{LM}$ and $\text{LM} + \text{M} \rightarrow \text{LM}_2$ ($\text{L} = \text{macrocycle}$, $\text{M} = \text{CF}_3\text{COOAg}$). The formation of complexes exceeding the 1/3 or 3/1 metal/macrocycle ratio was omitted for clarify.

In all cases, $\log K_1$ was larger than $\log K_2$, as shown in Table 3. The distributions of the [1/1 complex], [1/2 complex], $[\text{Ag}^+]$, and [macrocycle], in the cases of **1** and **5**, versus the amount of silver trifluoroacetate were derived from the binding constants (Figure 7). Similarly, the distributions of the [1/1 complex], [2/1 complex], $[\text{Ag}^+]$, and [macrocycle] for **2**, **3**, and **4** were derived. The distribution diagram showed that the 1,4-diselenin unit

TABLE 3. Binding Constants for Complexation of Unsaturated Selenacrown Ethers with CF_3COOAg in Acetone- d_6 at 25 °C

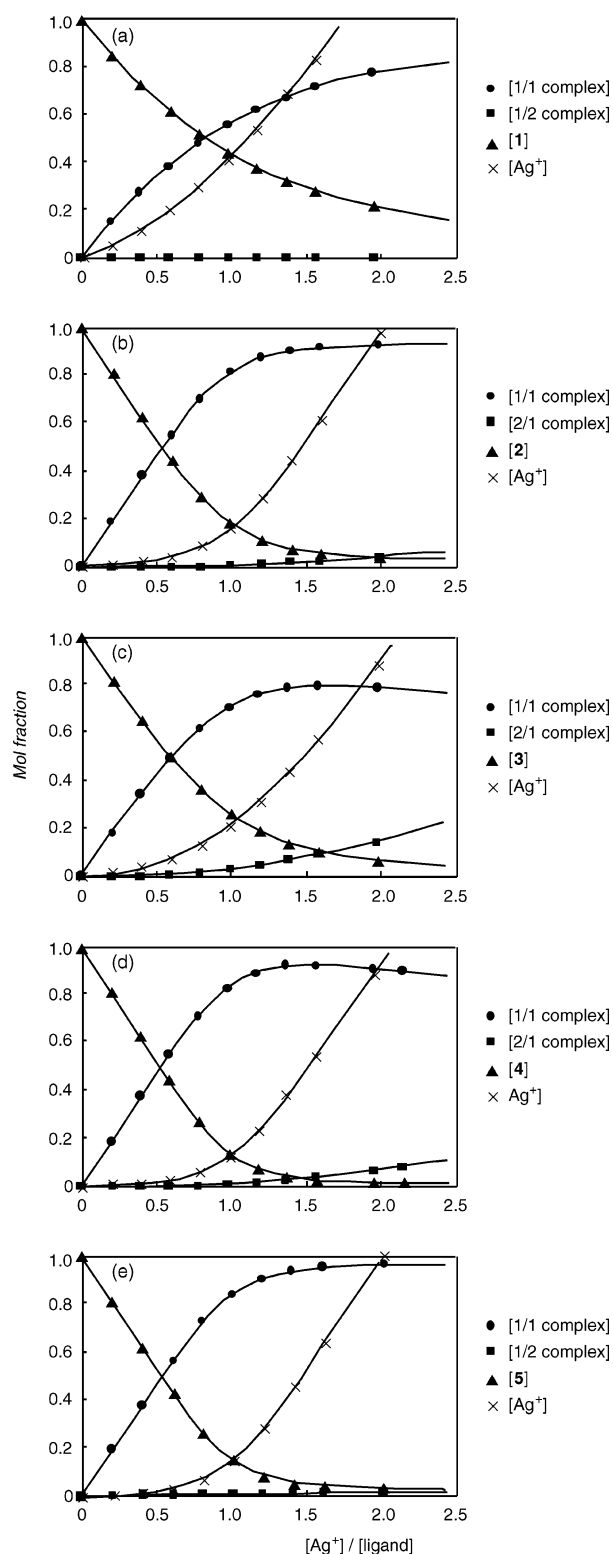
compd	$\log K_1$	$\log K_2$
1,4-diselenin (1)	3.9 ± 0.3	0.91 ± 0.2
15-US-5 (2)	5.2 ± 0.3	2.3 ± 0.2
18-US-6 (3)	4.6 ± 0.3	2.8 ± 0.2
21-US-7 (4)	6.0 ± 0.5	2.7 ± 0.4
24-US-8 (5)	5.3 ± 0.3	1.7 ± 0.1

exists almost entirely as a 1/1 complex in solution, in the case of **1**, although the 1/2 complex was also obtained as a solid. In the case of **2**, the 1/1 complex is formed, corresponding to the complex obtained as a solid. In the case of **3**, the 1/1 complex is the major product in solution. However, when the same procedure was performed for **3** at a concentration of 2.0 mM, the concentrations of the 1/1 and 2/1 complexes were almost the same at the point corresponding to the 2/1 ($[\text{Ag}^+]/[\mathbf{3}]$) ratio. This result corresponds well to the result that the crystal lattice was composed of a mixture of the macrocycles including either one or two silver atoms. Similarly, the 1/1 complexes of **4** and **5** were found to be formed mainly in solution. No clear evidence of an inflection point was observed in the titration curves of **4** and **5** at 2.0 mM. However, at 0.2 mM, a clear inflection point was observed for the two unsaturated selenacrown ethers. These results indicate that the 1/1 complexes exist mainly under the dilution conditions and additional complexation occurs at higher concentrations.

Electrochemistry of Silver Complexes with Unsaturated Selenacrown Ethers. The electrochemical redox behavior of complexes **9–14** was examined. The cyclic voltammograms were measured in acetonitrile with a Pt working electrode. All of the complexes exhibited irreversible oxidation peaks at +0.78, +0.77, +0.80, +0.73, +0.74, and +0.78 V vs Fc/Fc^+ and irreversible reduction peaks at -0.38, -0.34, -0.38, -0.32, -0.33, and -0.33 V, respectively, whereas silver trifluoroacetate showed only one irreversible reduction peak at -0.31 V. Comparing the oxidation and reduction potentials of the complexes with those of free macrocycles **2–5** and silver trifluoroacetate revealed that upon complexation with silver trifluoroacetate, the macrocycles become more resistant to oxidation, and, correspondingly, silver trifluoroacetate is less likely to be reduced upon complexation with the macrocycles.

Conclusions

Unsaturated selenacrown ethers (**2–6**) were synthesized, and their characterization and redox properties were clarified. X-ray analysis of **2–5** revealed that all of the selenium atoms lay almost on their respective planes and were oriented toward the cavities, and the molecular structures become elliptically slender with increasing ring size. The unsaturated selenacrown ethers were decomposed by heating to give 1,4-diselenin. Silver complexes of **1–5** were synthesized, and some of their structures were determined by X-ray crystallographic analysis. The silver ion inclusion behavior of the unsaturated selenacrown ethers was examined in solution. It was found that the unsaturated selenacrown ethers selectively formed 1/1 complexes at low concentration in solution.

**FIGURE 7.** Distribution diagram of complexation with Ag^+ for (a) **1**, (b) **2**, (c) **3**, (d) **4**, and (e) **5** ($[\text{macrocycle}]_t = 0.2 \text{ mM}$).

Experimental Section

Synthesis of Unsaturated Selenacrown Ethers. Selenium (7.1 g, 90 mmol), sodium hydroxide (11 g, 276 mmol), and rongalite (14 g, 90 mmol) were dissolved in 30 mL of water, and the mixture was sonicated for 15 min. Methanol (20 mL) was added to the reaction mixture, and the resulting sodium selenide (Na_2Se) was washed with 40 mL of acetonitrile four

times. Acetonitrile (650 mL) and 15-crown-5 (2.0 g, 9.1 mmol) were added to the sodium selenide. An acetonitrile solution (50 mL) of *cis*-dichloroethene (18 g, 0.18 mol) was added dropwise to the suspension with stirring during 1 h at room temperature. After additional stirring for 60 h, the resulting solids were filtered off, and the filtrate was concentrated in vacuo. The products were extracted with ethyl acetate (50 mL, 10 times) and dichloromethane (50 mL, five times), washed with water, and dried over magnesium sulfate. The products were isolated by silica gel column chromatography (hexane/acetone = 2/1), subsequently by gel permeation chromatography (chloroform).

1,4-Diselenin (1). bp 142 °C (yellow oil); ¹H NMR (500 MHz, CDCl₃) δ 7.04 (4H, s); ¹H NMR (500 MHz, DMSO-*d*₆) δ 7.12 (4H, s); ¹³C NMR (125 MHz, CDCl₃) δ 120.0; ¹³C NMR (125 MHz, DMSO-*d*₆) δ 120.1; ⁷⁷Se NMR (95 MHz, CDCl₃) δ 377.6; ⁷⁷Se NMR (95 MHz, DMSO-*d*₆) δ 372.1; MS (EI) *m/z* 212 (⁸⁰Se₂, M⁺, 48%), 186 (⁸⁰Se₂, M⁺ - C₂H₂, 19%), 160 (⁸⁰Se₂, 100%); IR (neat) ν_{\max} 3016, 1529, 1227, 722, 654 cm⁻¹; UV (MeCN) λ_{\max} 269 (ε 5.3 × 10³); (EtOH) λ_{\max} 271 (ε 4.6 × 10³); (CH₂Cl₂) λ_{\max} 274 (ε 4.4 × 10³); (C₆H₁₂) λ_{\max} 272 (ε 4.5 × 10³) nm. Anal. Calcd for C₄H₄Se₂: C, 22.88; H, 1.92. Found: C, 22.79; H, 1.92.

(Z,Z,Z,Z,Z)-1,4,7,10,13-Pentaselecyclopentadeca-2,5,8,11,14-pentaene (15-US-5) (2). mp 131.5–133.5 °C (colorless prisms from acetone-hexane); ¹H NMR (500 MHz, CDCl₃) δ 7.16 (10H, s); ¹H NMR (500 MHz, DMSO-*d*₆) δ 7.35 (10H, s); ¹³C NMR (125 MHz, CDCl₃) δ 127.0; ¹³C NMR (125 MHz, DMSO-*d*₆) δ 127.1; ⁷⁷Se NMR (95 MHz, CDCl₃) δ 336.5; ⁷⁷Se NMR (95 MHz, DMSO-*d*₆) δ 340.8; MS (FAB) *m/z* 526 (M⁺, ⁷⁸Se₂⁸⁰Se₃); IR (KBr) ν_{\max} 3004, 1531, 1246, 716, 677, 646 cm⁻¹; UV (MeCN) λ_{\max} 252 (ε 2.0 × 10⁴); (EtOH) λ_{\max} 259 (ε 1.5 × 10⁴); (CH₂Cl₂) λ_{\max} 260 (ε 2.2 × 10⁴); (C₆H₁₂) λ_{\max} 261 (ε 2.2 × 10⁴) nm. Anal. Calcd for C₁₀H₁₀Se₅: C, 22.88; H, 1.92. Found: C, 23.01; H, 1.89.

(Z,Z,Z,Z,Z,Z)-1,4,7,10,13,16-Hexaselenacyclooctadeca-2,5,8,11,14,17-hexaene (18-US-6) (3). mp 150.0–151.0 °C (colorless prisms from acetone-hexane); ¹H NMR (500 MHz, CDCl₃) δ 7.12 (12H, s); ¹H NMR (500 MHz, DMSO-*d*₆) δ 7.35 (12H, s); ¹³C NMR (125 MHz, CDCl₃) δ 125.7; ¹³C NMR (125 MHz, DMSO-*d*₆) δ 125.5; ⁷⁷Se NMR (95 MHz, CDCl₃) δ 350.1; ⁷⁷Se NMR (95 MHz, DMSO-*d*₆) δ 352.9; MS (FAB) *m/z* 632 (M⁺, ⁷⁸Se₂⁸⁰Se₄); IR (KBr) ν_{\max} 3014, 1539, 1239, 718, 644, 629 cm⁻¹; UV (MeCN) λ_{\max} 262 (ε 2.7 × 10⁴); (EtOH) λ_{\max} 266 (ε 1.9 × 10⁴); (CH₂Cl₂) λ_{\max} 269 (ε 2.8 × 10⁴); (C₆H₁₂) λ_{\max} 271 nm. Anal. Calcd for C₁₂H₁₂Se₆: C, 22.88; H, 1.92. Found: C, 22.95; H, 2.05.

(Z,Z,Z,Z,Z,Z,Z)-1,4,7,10,13,16,19-Heptaselecycloheptacos-2,5,8,11,14,17,20-heptaene (21-US-7) (4). mp 136.5–137.3 °C (colorless prisms from acetone-hexane); ¹H NMR (500 MHz, CDCl₃) δ 7.09 (14H, s); ¹H NMR (500 MHz, DMSO-*d*₆) δ 7.36 (14H, s); ¹³C NMR (125 MHz, CDCl₃) δ 124.8; ¹³C NMR (125 MHz, DMSO-*d*₆) δ 123.8; ⁷⁷Se NMR (95 MHz, CDCl₃) δ 353.7; ⁷⁷Se NMR (95 MHz, DMSO-*d*₆) δ 355.6; MS (FAB) *m/z* 736 (⁷⁸Se₃⁸⁰Se₄, M⁺); IR (KBr) ν_{\max} 3012, 1551, 1243, 716, 669, 618 cm⁻¹; UV (MeCN) λ_{\max} 251 (ε 3.8 × 10⁴); (EtOH) λ_{\max} 253 (ε 3.1 × 10⁴); (CH₂Cl₂) λ_{\max} 256 (ε 3.7 × 10⁴); (C₆H₁₂) λ_{\max} 266 nm. Anal. Calcd for C₁₄H₁₄Se₇: C, 22.88; H, 1.92. Found: C, 23.32; H, 2.00.

(Z,Z,Z,Z,Z,Z,Z,Z)-1,4,7,10,13,16,19,22-Octaselecyclo-tetracos-2,5,8,11,14,17,20,23-octaene (24-US-8) (5). mp 131.0–132.0 °C (yellow prisms from dichloromethane-hexane); ¹H NMR (500 MHz, CDCl₃) δ 7.08 (16H, s); ¹H NMR (500 MHz, DMSO-*d*₆) δ 7.37 (16H, s); ¹³C NMR (125 MHz, CDCl₃) δ 124.3; ¹³C NMR (125 MHz, DMSO-*d*₆) δ 123.0; ⁷⁷Se NMR (95 MHz, CDCl₃) δ 354.9; ⁷⁷Se NMR (95 MHz, DMSO-*d*₆) δ 357.5; MS (FAB) *m/z* 949 (⁷⁸Se₃⁸⁰Se₅, M⁺+¹⁰⁷Ag); IR (KBr) ν_{\max} 3015, 1560, 1235, 717, 677, 639 cm⁻¹; UV (MeCN) λ_{\max} 254 (ε 5.0 × 10⁴); (EtOH) λ_{\max} 261 (ε 3.9 × 10⁴); (CH₂Cl₂) λ_{\max} 262 (ε 4.7 × 10⁴); (C₆H₁₂) λ_{\max} 269 nm. Anal. Calcd for C₁₆H₁₆Se₈: C, 22.88; H, 1.92. Found: C, 22.86; H, 1.90.

(Z,Z,Z,Z,Z,Z,Z,Z,Z)-1,4,7,10,13,16,19,22,25-Nona-selenacycloheptacos-2,5,8,11,14,17,20,23,26-nonaene (27-US-9) (6). mp 137.5–138.5 °C (yellow prisms from dichloromethane); ¹H NMR (500 MHz, CDCl₃) δ 7.06 (18H, s); ¹³C NMR (125 MHz, CDCl₃) δ 123.8; ⁷⁷Se NMR (95 MHz, CDCl₃) δ 357.7; MS (FAB) *m/z* 1053 (⁷⁸Se₄⁸⁰Se₅, M⁺ + ¹⁰⁷Ag); IR (KBr) ν_{\max} 3014, 1559, 1539, 1235, 717, 677, 638 cm⁻¹; UV (MeCN) λ_{\max} 256 (ε 5.8 × 10⁴); (EtOH) λ_{\max} 262 (ε 4.6 × 10⁴); (CH₂Cl₂) λ_{\max} 264 (ε 5.5 × 10⁴); (C₆H₁₂) λ_{\max} 271 nm. Anal. Calcd for C₁₈H₁₈Se₉: C, 22.88; H, 1.92. Found: C, 22.98; H, 1.92.

Theoretical Study. Geometries were optimized using the Hartree-Fock (HF) method with the LANL2DZ basis set. The final energies were calculated by MP2 method using the HF geometries. All calculations were performed by using the Gaussian 98 program¹⁶ on an IBM p690-681 computer.

Thermal Reaction. In a sealed NMR tube, a solution of macrocycles (1.0 × 10⁻⁵ mol) in CDCl₃ (0.5 mL) or DMSO-*d*₆ (0.5 mL) was heated at 100 °C. The reactions were monitored by ¹H NMR measurement, and the yields of the products were also determined by ¹H NMR.

Synthesis of Silver Complexes of 1. An acetone solution (6 mL) of 1 or 0.5 equiv of silver trifluoroacetate was added to an acetone solution (6 mL) of 1 (0.4 mmol) under nitrogen. The reaction mixture was stirred at room temperature for 4 h. Crystallization by slow evaporation of acetone under N₂ stream yielded colorless crystals of Ag(C₄H₄Se₂)(CF₃COO) (7) or Ag(C₄H₄Se₂)₂(CF₃COO) (8), respectively.

Ag(C₄H₄Se₂)(CF₃COO) (7). 80%; mp 123.0 °C (colorless plates from acetone, decomp); ¹H NMR (500 MHz, DMSO-*d*₆) δ 7.20 (4H, s); ¹³C NMR (125 MHz, DMSO-*d*₆) δ 121.7, 158.5 (q, *J* = 31 Hz); ⁷⁷Se NMR (95 MHz, DMSO-*d*₆) δ 366.2; MS (FAB) *m/z* 319 (¹⁰⁷Ag⁸⁰Se₂, M⁺ - CF₃COO); IR (KBr) ν_{\max} 3020, 3001, 1686, 1208, 1135, 718, 700, 670, 650 cm⁻¹. Anal. Calcd for C₆H₄AgF₃O₂Se₂: C, 16.72; H, 0.94. Found: C, 16.68; H, 1.06.

Ag(C₄H₄Se₂)₂(CF₃COO) (8). 89%; mp 124.0 °C (colorless prisms from acetone, decomp); ¹H NMR (500 MHz, DMSO-*d*₆) δ 7.23 (8H, s); ¹³C NMR (125 MHz, DMSO-*d*₆) δ 121.4, 158.3 (q, *J* = 33 Hz); ⁷⁷Se NMR (95 MHz, DMSO-*d*₆) δ 367.0; MS (FAB) *m/z* 529 (¹⁰⁷Ag⁷⁸Se⁸⁰Se₃, M⁺ - CF₃COO); IR (KBr) ν_{\max} 3020, 3001, 1685, 1207, 1136, 718, 701, 670, 650 cm⁻¹. Anal. Calcd for C₁₀H₈AgF₃O₂Se₄: C, 18.74; H, 1.26. Found: C, 18.60; H, 1.30.

General Procedure for Synthesis of Silver Complexes of Unsaturated Selenacrown Ethers. An acetone solution (2 mL) of the desired amount of silver trifluoroacetate, silver nitrate, or silver tetrafluoroborate was added to an acetone solution (5–16 mL) of unsaturated selenacrown ethers 2–5 (0.05 mmol) under nitrogen. The reaction mixture was stirred at room temperature for 16, 14, 5, 4, 4, 4, 16, or 14 h for formation of 9–16, respectively. Crystallization by slow evaporation of acetone under N₂ stream yielded crystals or solids of silver complexes of unsaturated selenacrown ethers.

Ag(15-US-5)(CF₃COO) (9). 66%; mp 151.5 °C (colorless prisms from acetone-hexane, decomp); ¹H NMR (500 MHz, DMSO-*d*₆) δ 7.46 (10H, s); ¹³C NMR (125 MHz, DMSO-*d*₆) δ 128.2; ⁷⁷Se NMR (95 MHz, DMSO-*d*₆) δ 277.5; MS (FAB) *m/z* 633 (¹⁰⁷Ag⁷⁸Se₂⁸⁰Se₃, M⁺ - CF₃COO); IR (KBr) ν_{\max} 3005, 1683,

(16) Frisch, M. J.; Trucks, G. W.; Schlegel, H. B.; Scuseria, G. E.; Robb, M. A.; Cheeseman, J. R.; Zakrzewski, V. G.; Montgomery, J. A., Jr.; Stratmann, R. E.; Burant, J. C.; Dapprich, S.; Millam, J. M.; Daniels, A. D.; Kudin, K. N.; Strain, M. C.; Farkas, O.; Tomasi, J.; Barone, V.; Cossi, M.; Cammi, R.; Mennucci, B.; Pomelli, C.; Adamo, C.; Clifford, S.; Ochterski, J.; Petersson, G. A.; Ayala, P. Y.; Cui, Q.; Morokuma, K.; Salvador, P.; Dannenberg, J. J.; Malick, D. K.; Rabuck, A. D.; Raghavachari, K.; Foresman, J. B.; Cioslowski, J.; Ortiz, J. V.; Baboul, A. G.; Stefanov, B. B.; Liu, G.; Liashenko, A.; Piskorz, P.; Komaromi, I.; Gomperts, R.; Martin, R. L.; Fox, D. J.; Keith, T.; Al-Laham, M. A.; Peng, C. Y.; Nanayakkara, A.; Challacombe, M.; Gill, P. M. W.; Johnson, B.; Chen, W.; Wong, M. W.; Andres, J. L.; Gonzalez, C.; Head-Gordon, M.; Replogle, E. S.; Pople, J. A. *Gaussian 98*, revision A.11; Gaussian, Inc.: Pittsburgh, PA, 2001.

1247, 1208, 1129, 716, 689, 677, 647 cm^{-1} . Anal. Calcd for $\text{C}_{12}\text{H}_{10}\text{AgF}_3\text{O}_2\text{Se}_5$: C, 19.32; H, 1.35. Found: C, 19.36; H, 1.52.

Ag₅(18-US-6)₃(CF₃COO)₅ (10). 61%; mp 129.5 °C (yellow prisms from acetone-hexane, decomp); ¹H NMR (500 MHz, DMSO-*d*₆) δ 7.51 (36H, s); ¹³C NMR (125 MHz, DMSO-*d*₆) δ 117.5 (q, *J* = 286 Hz), 126.9, 158.1 (q, *J* = 31 Hz); ⁷⁷Se NMR (95 MHz, DMSO-*d*₆) δ 315.7; MS (FAB) *m/z* 961 (¹⁰⁷Ag¹⁰⁹Ag⁷⁸Se₂⁸⁰Se₄, **2** + CF₃COOAg₂), 739 (¹⁰⁷Ag⁷⁸Se₂⁸⁰Se₄, (**2** + Ag)⁺); IR (KBr) ν_{max} 3014, 1683, 1239, 1207, 1132, 718, 644, 628 cm^{-1} . Anal. Calcd for $\text{C}_{46}\text{H}_{36}\text{Ag}_5\text{F}_{15}\text{O}_{10}\text{Se}_{18}$: C, 18.45; H, 1.21. Found: C, 18.41; H, 1.27.

Ag₇(21-US-7)(CF₃COO)₅(Me₂CO)₃ (11). 2%; mp 123.5 °C (yellow prisms from acetone-hexane, decomp); ¹H NMR (500 MHz, DMSO-*d*₆) δ 7.39 (14H, s); ¹³C NMR (125 MHz, DMSO-*d*₆) δ 124.7; ⁷⁷Se NMR (95 MHz, DMSO-*d*₆) δ 334.6; MS (FAB) *m/z* 952 (¹⁰⁷Ag¹⁰⁹Ag⁷⁸Se₃⁸⁰Se₄, **4** + Ag₂), 843 (¹⁰⁷Ag⁷⁸Se₃⁸⁰Se₄, **4** + Ag); IR (KBr) ν_{max} 3017, 1674, 1239, 1208, 1136, 839, 806, 725 cm^{-1} . Anal. Calcd for $\text{C}_{33}\text{H}_{32}\text{Ag}_7\text{F}_{15}\text{O}_{13}\text{Se}_7$: C, 17.78; H, 1.45. Found: C, 17.66; H, 1.19.

Ag(24-US-8)₂(CF₃COO) (12). 36%; mp 70.0 °C (colorless powder from acetone, decomp); ¹H NMR (500 MHz, DMSO-*d*₆) δ 7.42 (32H, s); ¹³C NMR (125 MHz, DMSO-*d*₆) δ 119.4 (q, *J* = 296 Hz), 124.4; ⁷⁷Se NMR (95 MHz, DMSO-*d*₆) δ 346.6; MS (FAB) *m/z* 949 (¹⁰⁷Ag⁷⁸Se₃⁸⁰Se₅, **5** + Ag); IR (KBr) ν_{max} 3015, 1679, 1237, 1198, 1126, 716, 676 cm^{-1} . Anal. Calcd for $\text{C}_{34}\text{H}_{32}\text{Ag}_2\text{F}_3\text{O}_2\text{Se}_{16}$: C, 21.48; H, 1.70. Found: C, 21.39; H, 1.90.

Ag₂(24-US-8)(CF₃COO)₂ (13). 51%; mp 144.5 °C (colorless prisms from acetone, decomp); ¹H NMR (500 MHz, DMSO-*d*₆) δ 7.43 (16H, s); ¹³C NMR (125 MHz, DMSO-*d*₆) δ 117.4 (q, *J* = 289 Hz), 124.7, 158.2 (q, *J* = 31 Hz); ⁷⁷Se NMR (95 MHz, DMSO-*d*₆) δ 343.0; MS (FAB) *m/z* 1171 (¹⁰⁷Ag¹⁰⁹Ag⁷⁸Se₃⁸⁰Se₅, M⁺ - CF₃COO) 949 (¹⁰⁷Ag⁷⁸Se₃⁸⁰Se₅, **5** + Ag); IR (KBr) ν_{max} 3015, 1657, 1235, 1198, 1128, 721, 712, 677, 624 cm^{-1} . Anal. Calcd for $\text{C}_{20}\text{H}_{16}\text{Ag}_2\text{F}_6\text{O}_4\text{Se}_8$: C, 18.74; H, 1.26. Found: C, 18.76; H, 1.29.

Ag₃(24-US-8)₂(CF₃COO)₃ (14). 20%; mp 134.5 °C (colorless prisms from acetone, decomp); ¹H NMR (500 MHz, DMSO-*d*₆) δ 7.46 (32H, s); ¹³C NMR (100 MHz, DMSO-*d*₆) δ 125.3; ⁷⁷Se NMR (95 MHz, DMSO-*d*₆) δ 338.1; MS (FAB) *m/z* 1171 (¹⁰⁷Ag¹⁰⁹Ag⁷⁸Se₃⁸⁰Se₅, **5** + CF₃COOAg₂), 949 (¹⁰⁷Ag⁷⁸Se₃⁸⁰Se₅, **5** + Ag); IR (KBr) ν_{max} 3015, 1683, 1237, 1207, 1131, 716, 674, 642 cm^{-1} . Anal. Calcd for $\text{C}_{38}\text{H}_{32}\text{Ag}_3\text{F}_9\text{O}_6\text{Se}_8$: C, 19.48; H, 1.38. Found: C, 19.66; H, 1.44.

Ag(15-US-5)NO₃ (15). 49%; mp 122.5 °C (colorless prisms from acetone-methanol, decomp); ¹H NMR (500 MHz, DMSO-*d*₆) δ 7.45 (10H, s); MS (FAB) *m/z* 633 (¹⁰⁷Ag⁷⁸Se₂⁸⁰Se₃, M⁺ - CF₃COO); IR (KBr) ν_{max} 3010, 1385, 1312, 695, 670 cm^{-1} . Anal. Calcd for $\text{C}_{10}\text{H}_{10}\text{AgNO}_3\text{Se}_5$: C, 17.29; H, 1.45; N, 2.02. Found: C, 17.31; H, 1.43; N, 2.01. The ¹³C and ⁷⁷Se NMR could not be measured due to insolubility of **15** in suitable solvents.

Ag(21-US-7)BF₄ (16). 91%; mp 147.0 °C (colorless powder from acetone, decomp); ¹H NMR (500 MHz, DMSO-*d*₆) δ 7.40

(14H, s); ¹³C NMR (125 MHz, DMSO-*d*₆) δ 124.5; ⁷⁷Se NMR (95 MHz, DMSO-*d*₆) δ 374.7; MS (FAB) *m/z* 843 (¹⁰⁷Ag⁷⁸Se₃⁸⁰Se₄, M⁺ - BF₄); IR (KBr) ν_{max} 3014, 1551, 1244, 1063, 1035, 716, 667, 619 cm^{-1} . Anal. Calcd for $\text{C}_{14}\text{H}_{14}\text{AgBF}_4\text{Se}_7$: C, 18.09; H, 1.52. Found: C, 18.33; H, 1.60.

Typical Procedure for ¹H NMR Shift Titration. To an acetone-*d*₆ solution of macrocycle (5×10^{-4} M, 200 μL) in an NMR tube were added required amounts of acetone-*d*₆ solution of CF₃COOAg (4×10^{-4} M, 0–175 μL) individually. The volume of the samples was prepared to 500 μL by addition of acetone-*d*₆ (concentration of macrocycle = 2×10^{-4} M). ¹H NMR measurement of the samples was carried out at 25 °C.

Cyclic Voltammetry. Cyclic voltammograms were measured in acetonitrile. A 0.1 M solution of tetra-*n*-butylammonium perchlorate was used as supporting electrolyte solution. The solid samples were added and dissolved in this solution to yield 1.5 mM concentrations of the respective materials. Cyclic voltammograms were recorded at scan rate of 100 mV s⁻¹. Formal oxidation potentials are given versus the reference system ferrocene/ferrocenium (Fc/Fc⁺) in volts.

X-ray Structure Determination. The crystals of **4** and **5** were mounted on the end of a glass fiber, and the data collections were carried out on a Rigaku AFC7R diffractometer equipped with graphite-monochromated Mo K α ($\lambda = 0.71069$ Å) radiation. The crystal data of **8**–**10**, **13**, and **15** were collected by a Rigaku RAXIS-RAPID imaging plate two-dimensional area detector using graphite-monochromated Mo K α radiation ($\lambda = 0.71070$ Å) to 2 θ max of 55.0°. All of the crystallographic calculations were performed by using teXan software package of the Molecular Structure Corp. The X-ray structure was solved by the direct methods and refined by the full-matrix least squares. All non-hydrogen atoms were refined anisotropically.

Acknowledgment. This work was financially supported in part by a Grant-in-Aid for Scientific Research from the Ministry of Education, Science, Sports, Culture, Japan. We thank Dr. K. Sato and Professor T. Yamagishi (Tokyo Metropolitan University) for measurement of FAB MS and useful advice and discussion on the determination of binding constants.

Supporting Information Available: X-ray crystallographic files (CIF) for **4**, **5**, **8**, **9**, **13**, and **15**. Summarized tables of X-ray crystallographic data and selected atomic distances and angles. The Cartesian coordinates of optimized structures of 6-, 9-, 12-, 15-, 18-, 21-, 24-, and 27-membered unsaturated selenacrown ethers. This material is available free of charge via the Internet at <http://pubs.acs.org>.

JO0502807